

In silico study and *in vitro* antileishmanial and antitrypanosomal evaluation of azopyrazoles and azopyrimidines

Abdulsalam AM Alkhaldi¹, Phoebe F Lamie² and Mohamed A Abdelgawad^{3*}

¹Department of Biology, College of Science, Jouf University, Sakaka, Saudi Arabia

²Pharmaceutical Organic Chemistry Department, Faculty of Pharmacy, Beni-Suef University, Beni-Suef, Egypt

³Department of Pharmaceutical Chemistry, College of Pharmacy, Jouf University, Sakaka, Saudi Arabia

Abstract: Hydrazones 1-6, azo-pyrazoles 7-9 and azo-pyrimidines 10-15 are compounds that exhibit antibacterial activity. The mode of action and structures of these derivatives have been previously confirmed as antibacterial. In this investigation, biological screening and molecular docking studies were performed for derivatives 1-15, with compounds 2, 7, 8, 14 and 15 yielding the best energy scores (from -20.7986 to -10.5302 kcal/mol). Drug-likeness and *in silico* ADME prediction for the most potent derivatives, 2, 7, 8, 14 and 15, were predicted (from 84.46 to 96.85%). The latter compounds showed good recorded physicochemical properties and pharmacokinetics. Compound 8 demonstrated the strongest inhibition, which was similar to the positive control (eflornithine) against *Trypanosoma brucei brucei* (WT), with an EC₅₀ of 25.12 and 22.52 μM, respectively. Moreover, compound 14 exhibited the best activity against *Leishmania mexicana* promastigotes and *Leishmania major* promastigotes (EC₅₀ =46.85; 40.78 μM, respectively).

Keywords: Pyrazole, pyrimidine, trypanosome, leishmania, docking.

INTRODUCTION

Neglected tropical diseases (NTDs) encompass several significant illnesses, with sleeping sickness human African trypanosomiasis; (HAT), Chagas disease (American trypanosomiasis) and leishmaniasis being particularly prominent (De Rycker *et al.*, 2018; Santos *et al.*, 2020; Kourbeli *et al.*, 2021). In Africa, HAT and leishmaniasis coexist, but in South America, Chagas disease and leishmaniasis are produced from similar trypanosomatid protozoan parasites (De Rycker *et al.*, 2018; Santos *et al.*, 2020; Kourbeli *et al.*, 2021). African trypanosomiasis continues to pose a threat to both human and animal populations due to the absence of effective treatments, drug toxicity and drug resistance. This underscores the need for a deeper understanding of the biology of parasites and the development of novel therapeutic interventions. Animal African trypanosomiasis and HAT are two types of the same neglected tropical disease, presenting significant hazards to both humans and animals in endemic areas (Cayla *et al.*, 2019; Franco *et al.*, 2019). It is projected that between 2016 and 2020, approximately 55 million individuals across sub-Saharan Africa will be susceptible to HAT; it is a fatal condition if it is left untreated (World Health Organization, 2020). Notably, the number of cases (animal African trypanosomiasis and HAT infection) has substantially declined in the previous few years (in 2019 and 2020, 992 and 663 new cases were verified, respectively) compared with those recorded in 1998 (~40,000 cases). Multiple control measures have contributed to this remarkable reduction; nevertheless, the disease has not been eradicated (Giordani *et al.*, 2016; Tihon *et al.*, 2017; Dize

et al., 2022). The presence of antigenic diversity among trypanosomes hinders the development of a viable vaccine, rendering chemotherapy the primary treatment approach (Black and Mansfield, 2016). However, the currently available drugs are associated with significant risks due to their toxicity, undesirable side effects, and decreasing efficacy due to the emergence of drug resistance. Consequently, there is a crucial need for development and research efforts to explore novel, highly effective, and safe treatments for trypanosomiasis (Black and Mansfield, 2016).

Leishmaniasis is a highly contagious and often fatal parasitic protozoal illness. It is primarily transmitted through the bites of infected insects in warm and humid environments (Rasheed *et al.*, 2019; Oliveira *et al.*, 2021). The clinical indicators of leishmaniasis can be categorized into two forms, with the cutaneous form (CL) being the most prevalent worldwide. CL severely affects the skin, hindering normal activities and presenting a significant healthcare challenge. *Leishmania tropica* and *Leishmania major* (*L. major*) are the primary species responsible for most CL cases globally. The sand fly, *Phlebotomus papatasi*, which is prevalent in regions with a high incidence of *L. major* infections, is thought to be the main contributor to the disease in Arabian countries, including Saudi Arabia (Khan *et al.*, 2023). CL (zoonotic form) resulted from the global expansion of leishmaniasis in the 20th century, with an estimated annual incidence of >4,000 cases in Saudi Arabia (Ghatee *et al.*, 2020; Khan *et al.*, 2021). CL's endemic nature in numerous regions of Saudi Arabia can be attributed to the widespread presence of sand flies and desert rodents (reservoir animals) (Abuzaid *et al.*, 2020; Alanazi *et al.*, 2021). Recent research conducted in the Qassim province of Central

*Corresponding author: e-mail: abdul salam@ju.edu.sa

MATERIALS AND METHODS

Chemistry

Elemental analysis, mass spectroscopy, IR and NMR spectroscopy and a melting point assessment were conducted in agreement with previously reported methods. The chemicals used were bought from Aldrich Chemical (Milwaukee, WI).

The used methods for the preparation of objective derivatives have been previously reported (Alkhalidi *et al.*, 2018; Abdegawad, 2019; Alkhalidi *et al.*, 2019; Oldenburg *et al.*, 2021).

General method for preparation of 1-6

To a mixture of aniline derivative (0.02 mol), HCl (20%, 5 ml) (ice cooled), an ice-cooled NaNO₂ (0.02 mol) solution was added portion-wise for over 30 mins and stirred to yield diazonium salt. To an ice-cooled solution of active methylene compounds (dicarbonyl) (0.02 mol) and CH₃COONa (0.04 mol) in C₂H₅OH (60%, 40 ml), diazonium salt was added and stirred for 3 h. The formed precipitate was filtered and crystallized from CH₃OH to yield derivatives 1 to 6

General method for preparation of 7-9

Compounds 1-3 (0.3mol, C₂H₅OH, 40ml) and PhNHNH₂ (0.35 mol) were heated under reflux for 12h. The precipitate at zero °C was filtered, dried and crystallized from acetic acid to yield compounds 7-9.

General method for preparation of 10-15

Ethoxide solution (Na, 0.06mol and C₂H₅OH 40ml) was combined with compounds 4-6 (0.02mol, in C₂H₅OH 40 ml). A mixture of urea or thiourea solution (0.02mol, ethanol 20ml) and the reaction mixture were subjected to reflux for 4 hours. Subsequently, hot water (80ml) was introduced, followed by the addition of HCl until the mixture exhibited acidity indicated by litmus paper. The resulting mixture was refrigerated for 2hours. The product was filtered, dried and subjected to crystallization from ethanol, resulting in the formation of compounds 10-15.

Biological screening (Antileishmanial and Antitrypanosomal Activities)

Cell culture

Trypanosoma brucei bloodstream forms *in vitro*

The bloodstream samples containing strains of *Trypanosoma brucei* were used to test the selected compounds. A wild-type strain of *Trypanosoma brucei* (Lister s427-WT), which is drug-sensitive, was used. HMI-9 medium (pH 7.4) was prepared and supplemented with 14µL/L of 13.4 M β-mercaptoethanol (Sigma) and 10% heat-inactivated fetal calf serum (BioSera) as described by Hirumi and Hirumi (1989). Subsequently, the culture medium was sterilized through filtration in a flow cabinet. Next, the cells were cultured on this

medium in an incubator at 37°C with 5% CO₂. Notably, the cells were passed in vented flasks thrice per week.

Leishmania mexicana and *Leishmania major* promastigotes

L. mexicana (strain MNYC/BZ/62/M379) and *L. major* strain Friedlin were cultured in medium (HOMEM) with 10% fetal calf serum (pH 7.4) in plastic flasks at 25°C. Cultures underwent medium renewal thrice weekly, following established protocols (Alzahrani *et al.*, 2017).

Alamar blue assay

The Alamar blue assay was used to assess the EC₅₀ of *Leishmania* and African trypanosomes cultures to the test candidates *in vitro*, along with positive controls (Eflornithine and Pentamidine), following procedures outlined in Alkhalidi *et al.*, (2019), Amisigo *et al* (2019). And Dias-Lopes *et al* (2021).

Molecular docking study

Molecular docking study was performed using MOE (Molecular Operating Environment 2014.0901) software. The crystal structure of flavin-adenin dinucleotide (FAD) bound at trypanothione reductase, from *Leishmania infantum*, active site was downloaded from Protein Data Bank, [(PDB) identifier: 2JK6]. For docking protocol, the first step was the protein preparation through; removing water molecules, adding hydrogen atoms and adopting potential energy by using the MMFF94x force field. In order to validate the docking protocol, the co-crystallized ligand (FAD) was energy minimized and saved as (mdb) file format. It docked inside the protein active site. The most stable docking pose was selected and the binding energy score, interaction type and bond length, as well as the relative mean square deviation (rmsd =1.7) were determined.

Secondly, the test compounds were drawn using Chem Draw Professional 16.0 and saved as (mol) file format. A library of compounds using MOE software was constructed. All test compounds were subjected to energy minimization then saved as (mdb) file format. The prepared compounds were then docked inside the trypanothione reductase active site. For each docked compound, the best superimposed pose with the ligand (FAD) was chosen. The energy score and the binding interactions with the amino acid residues of the active site were detected and represented in 2D and 3D pictures.

Predicted molecular properties and drug likeness

Drug-likeness properties of the most biologically active derivatives were assessed using molinspiration (2018.02 version), (<https://www.molinspiration.com/>), (supplementary data) Various molecular properties, including molecular weight (MW), hydrogen bond acceptors (nON), hydrogen bond donors (nOHNH), partition coefficient (logP), rotatable bonds (nrotb),

topological polar surface area (TPSA), molecular volume (MV), absorption percentage (% Abs) ($\% \text{Abs} = 109 - (0.345 \times \text{TPSA})$) and violation of Lipinski's rule of five (n-violation), were evaluated. Acceptable values and predicted results for target compounds and reference drugs are detailed in table 4.

In silico ADME prediction

PreADME online server (<https://preadmet.webservice.bmdrc.org/adme/>) was used to predict the in silico ADME properties of the most active derivatives, 2, 7, 8, 14 and 15 and the reference drug, Pentamidine. (Supplementary data)

Human intestinal absorption (HIA), the gastro-intestinal cell permeability of CaCo-2 cells and Maden Darby Canine Kidney (MDCK) cells, plasma protein binding (PPB), blood-brain barrier (BBB) and skin permeability (SP) parameters were measured and the obtained results are recorded.

Predicted molecular properties and drug likeness

Drug-likeness properties of the most biologically active derivatives were assessed using molinspiration (2018.02 version), (<https://www.molinspiration.com/>) (table 4).

In silico ADME prediction

PreADME online server (<https://preadmet.webservice.bmdrc.org/adme/>) was used to predict the in silico ADME properties of the most active derivatives, 2, 7, 8, 14 and 15, and the reference drug, Pentamidine (See Supplementary data).

STATISTICAL ANALYSIS

The data obtained from the study were analyzed using SPSS software version 26, employing the paired Student's t-test to assess the significance of EC₅₀ among various compounds and positive controls.

RESULTS

Chemistry

Azo-pyrazole, azo-pyrimidine and azo-oxo butyric acid derivatives were prepared according to previously reported methods (Abdegawad, 2019; Alkhaldi *et al.*, 2019) and outlined in scheme 1. The structure elucidation of the prepared derivatives was done through the known melting points and physical characters.

Biological screening

All compounds were tested for activities but only compounds which showed the highest binding energy scores, hydrazinelydine derivative 2, pyrazolone derivatives 7, 8 and thiopyrimidinone derivatives 14 and 15 were also, have moderate activity against of *L. major*, *L. mexicana* and *T. brucei* (s427-WT) *in vitro* using the Alamar Blue assay method. The antitrypanosomal and

antileishmanial activities of the target derivatives are listed in table 2.

Antitrypanosomal activity

Compounds 2, 7, 8, 14 and 15, demonstrated activity against *T. brucei*. Compounds 7 and 14 exhibited moderate activity against the parasites, while compound 15 displayed a lower activity level, with an EC₅₀ value of 80.83 μM . Interestingly, compound 8 showed significant activity against *Trypanosoma brucei*, with an EC₅₀ of 25.12 μM , which was comparable to that of the positive control (eflornithine) (i.e., EC₅₀ = 22.52 μM). According to the paired Student's *t*-test, the difference between them was not statistically significant.

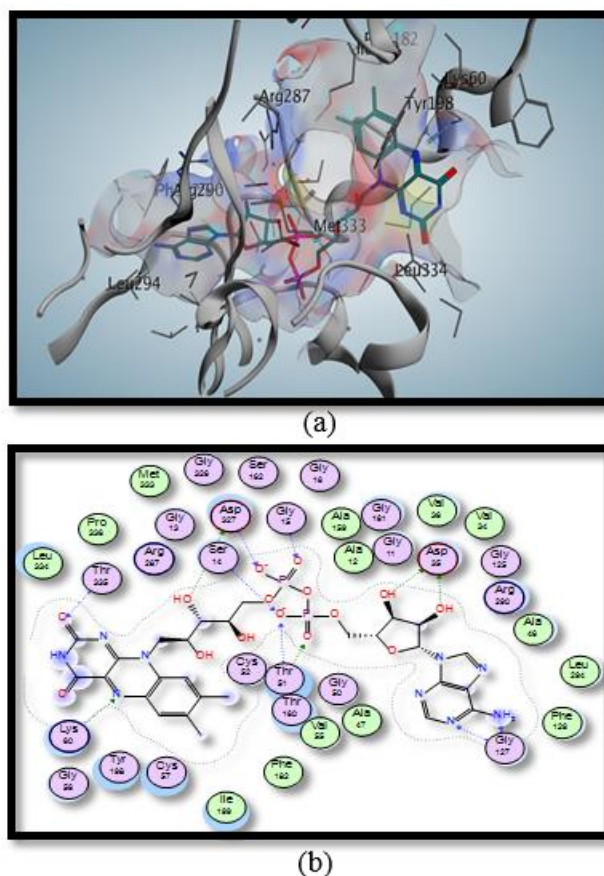


Fig. 2: View of the ligand compound (flavin-adenine dinucleotide) in the active site of the target protein (PDB-2JK6) with its amino acid residues: (a) three-dimensional view and (b) two-dimensional view.

Antileishmanial activity

Of all the tested compounds, only compounds 14 and 15 inhibited both *L. major* and *L. mexicana*. Compound 14 displayed moderate activity, with EC₅₀ values of 40.78 μM and 46.85 μM against *L. major* and *L. mexicana*, respectively. Compound 15 exhibited less potent activity, with EC₅₀ values ranging from 81 to 93 μM against both strains. Compounds 2, 7 and 8 did not show activity against the *Leishmania* species (table 2).

Table 1: Target compounds names and structures

| No. | R | R ¹ | Name |
|-----|---|----------------------------------|--|
| 1 | 4-COOC ₂ H ₅ | COCH ₃ | ethyl (E)-4-(2-(1-ethoxy-1,3-dioxobutan-2-ylidene)hydrazinyl)benzoate |
| 2 | 3-OCH ₃ , 4-OCH ₃ | COCH ₃ | ethyl (E)-2-(2-(3,4-dimethoxyphenyl)hydrazono)-3-oxobutanoate |
| 3 | 3-Cl, 4-Cl | COCH ₃ | ethyl (E)-2-(2-(3,4-dichlorophenyl)hydrazono)-3-oxobutanoate |
| 4 | 4-COOC ₂ H ₅ | COOC ₂ H ₅ | diethyl 2-(2-(4-(ethoxycarbonyl)phenyl)hydrazono)malonate |
| 5 | 3-OCH ₃ , 4-OCH ₃ | COOC ₂ H ₅ | diethyl 2-(2-(3,4-dimethoxyphenyl)hydrazono)malonate |
| 6 | 3-Cl, 4-Cl | COOC ₂ H ₅ | diethyl 2-(2-(3,4-dichlorophenyl)hydrazono)malonate |
| 7 | 4-COOC ₂ H ₅ | -- | ethyl (E)-4-(2-(3-methyl-5-oxo-1-phenyl-1,5-dihydro-4H-pyrazol-4-ylidene)hydrazinyl)benzoate |
| 8 | 3-OCH ₃ , 4-OCH ₃ | -- | (E)-4-(2-(3,4-dimethoxyphenyl)hydrazono)-5-methyl-2-phenyl-2,4-dihydro-3H-pyrazol-3-one |
| 9 | 3-Cl, 4-Cl | -- | (E)-4-(2-(3,4-dichlorophenyl)hydrazono)-5-methyl-2-phenyl-2,4-dihydro-3H-pyrazol-3-one |
| 10 | 4-COOC ₂ H ₅ | - | ethyl 4-(2-(2,4,6-trioxotetrahydropyrimidin-5(2H)-ylidene)hydrazinyl)benzoate |
| 11 | 3-OCH ₃ , 4-OCH ₃ | - | 5-(2-(3,4-dimethoxyphenyl)hydrazono)pyrimidine-2,4,6(1H,3H,5H)-trione |
| 12 | 3-Cl, 4-Cl | - | 5-(2-(3,4-dichlorophenyl)hydrazono)pyrimidine-2,4,6(1H,3H,5H)-trione |
| 13 | 4-COOC ₂ H ₅ | - | ethyl 4-(2-(4,6-dioxo-2-thioxotetrahydropyrimidin-5(2H)-ylidene)hydrazinyl)benzoate |
| 14 | 3-OCH ₃ , 4-OCH ₃ | - | 5-(2-(3,4-dimethoxyphenyl)hydrazono)-2-thioxodihydropyrimidine-4,6(1H,5H)-dione |
| 15 | 3-Cl, 4-Cl | - | 5-(2-(3,4-dichlorophenyl)hydrazono)-2-thioxodihydropyrimidine-4,6(1H,5H)-dione |

Table 2: Effect of compounds on *T. brucei*, *L. major* and *L. mexicana*.

| Compounds | <i>T. brucei</i> (WT) EC ₅₀ μM | <i>L. major</i> , promastigotes EC ₅₀ μM | <i>L. mexicana</i> , promastigotes EC ₅₀ μM |
|--------------|---|---|--|
| 1 | >100 | >100 | >100 |
| 2 | 35.89 ± 2.54 | >100 | >100 |
| 3 | >100 | >100 | >100 |
| 4 | >100 | >100 | >100 |
| 5 | >100 | >100 | >100 |
| 6 | >100 | >100 | >100 |
| 7 | 51.74 ± 0.51 | >100 | >100 |
| 8 | 25.12 ± 2.21 | >100 | >100 |
| 9 | >100 | >100 | >100 |
| 10 | >100 | >100 | >100 |
| 11 | >100 | >100 | >100 |
| 12 | >100 | >100 | >100 |
| 13 | >100 | >100 | >100 |
| 14 | 46.61 ± 0.77 | 40.780 ± 4.845 | 46.85 ± 0.15 |
| 15 | 80.83 ± 11.28 | 81.477 ± 9.172 | 93.72 ± 1.38 |
| Eflornithine | 22.52 ± 2.74 | ----- | ----- |
| Pentamidine | 0.005 ± 0.0001 | 4.340 ± 0.172 | 1.247 ± 0.113 |

In silico molecular docking studies

Concerning the results obtained from the docking on *Leshmania* species, *L. major* and *L. Mexicana* protein active site, table 3, it was observed that, the co-crystallized ligand, flavin-adenine dinucleotide (FAD), exerted 12 hydrogen bond interactions with ASP 35, GLY 127, ASP 327, THR 51, SER 14, GLY 127, THR 335, LYS 60 and GLY 15 amino acid residues with a docking score of -20.7986 kcal/mol (figs. 2a&b).

According to the data obtained from the docking of target compounds 2, 7, 8, 14 and 15 (supplementary data; table 3, and fig. 2-7), the docking scores ranged from -14.2566 to -9.0195 kcal/mol (table 3).

Compounds 2, 7, 8, and 14 exhibited the most significant energy binding scores (-12.6233, -13.3816, -14.2566 and -12.6970 kcal/mol, respectively) and formed up to two hydrogen bond interactions with THR 51, THR 335, ASP 327 and LYS 60 amino acid residues. These were the same amino acid residues involved in the same kind of hydrogen bonding interactions between the ligand (FAD) and the active site of the target protein.

Regarding docking study on oxidoreductase enzyme of *Trypanosome burcei*, (table 3, fig. 8-13), the crystal structure of the enzyme with the co-crystallized ligand, 3-chloro-4,6-dihydroxy-5-[(2E,6E,8S)-8-hydroxy-3,7-dimethylnona-2,6-dien-1-yl]-2-methylbenzaldehyde, was downloaded from pdb, ID identifier: 3VVa [<https://www.rcsb.org/structure/3vva>].

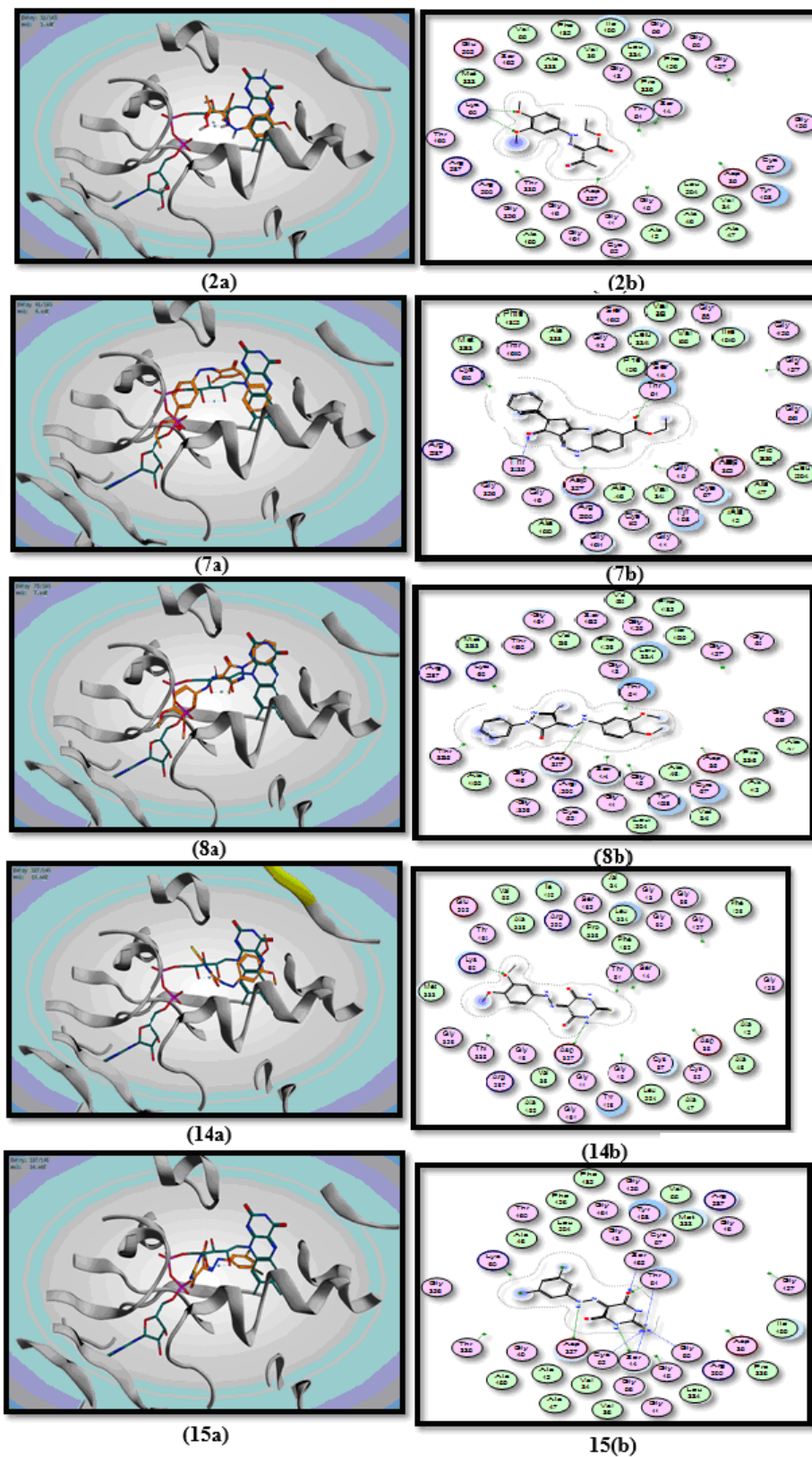


Fig. 3-7: (a) Superimposed view of target compound 2,7,8,14 and 15 (orange lines) and ligand molecule (cyan lines) in the active site of the target protein. (b) Two-dimensional view of hydrogen bonding interactions of compound 2,7,8,14 and 15 and in the active site amino acid residues of the target protein.

Table 3: Docking analysis (energy scores, binding interactions, and amino acid residues) of target compounds, 2, 7, 8, 14, 15 and the co-crystallized ligands of PDB-2JK6 and 3VVa.

| No. | PDB-2JK6 | | | PDB-3VVa | | |
|--------|--------------------|---|---|--------------------|-------------------------------------|---|
| | E-score (kcal/mol) | Binding interactions | Amino acid residues with distances (Å) | E-score (kcal/mol) | Binding interactions | Amino acid residues with distances (Å) |
| Ligand | -20.7986 | OH OH NH ₂ OH P=O P-O ⁻ P-O ⁻ Pyrimidine N C=O Quinazoline N P=O P-O ⁻ | ASP 35 (2.43), ASP 35 (2.60), GLY 127 (2.83), ASP 327 (2.52), THR 51 (2.37), SER 14 (3.53), THR 51(2.76), GLY 127 (2.79), THR 335 (2.72), LYS 60 (2.90), GLY 15 (2.62), ASP 327 (2.70) | -10.4465 | OH C=O OH | Glu 213 (2.30) ARG 118 (2.55) MET 190 (3.39) |
| 2 | -12.6233 | OCH ₃ OCH ₃ | LYS 60 (2.81), LYS 60 (2.87) | -8.9444 | pi-H | LEU 122 (4.14) |
| 7 | -13.3816 | C=O C=O (-COOEt) | THR 335 (3.16), THR 51 (2.61) | -7.9950 | pi-H pi-cation | LEU 122 (4.18) ARG 118 (4.69) |
| 8 | -14.2566 | NH | ASP 327 (3.03) | -10.2820 | pi-H | LEU 122 (4.37) |
| 14 | -12.6970 | NH OCH ₃ | ASP 327 (2.47), LYS 60 (2.63) | -9.8561 | pi-H | ARG 96 (4.02) |
| 15 | -10.5302 | NH C=O C=O C=O NH C=O C=O C=O | ASP 327 (3.14), SER 14 (3.21), THR 51 (2.94), SER 162 (3.09), SER 14 (2.83), GLY 50 (3.50), THR 51 (3.10), CYS 52 (3.15) | -8.9668 | C=O N=NH Pyrimidine-NH C=S | ARG 118 (3.28) ARG 118 (3.16) GLU 213 (3.28) GLU 123 (4.42) |

Table 4: Predicted properties and Lipinski parameters for target compounds 2, 7, 8, 14 and 15 compared with those of the reference drug, Pentamidine. ^aMolecular weight. ^bNumber of hydrogen-bond acceptors. ^cNumber of hydrogen-bond donors. ^dOctanol/ water partition coefficient. ^eNumber of rotatable bonds. ^fTopological polar surface area. ^gMolecular volume. ^hPercentage of absorption (%Abs = 109 -[0.345 × TPSA]).

| Compd. No. | ^a MW | ^b nON | ^c nOHNH | ^d logP (o/w) | ^e nrotb | ^f TPSA | ^g MV | ^h % Abs | n-violation |
|------------------|-----------------|------------------|--------------------|-------------------------|--------------------|-------------------|-----------------|--------------------|-------------|
| Acceptable value | <500 | <10 | <5 | <5 | ≤10 | <160 | 500 | 100% | ≤1 |
| 2 | 292.29 | 7 | 1 | 2.60 | 8 | 86.23 | 262.04 | 79.26 | 0 |
| 7 | 350.38 | 7 | 1 | 3.27 | 6 | 85.59 | 313.19 | 79.48 | 0 |
| 8 | 338.37 | 7 | 1 | 2.37 | 5 | 77.76 | 302.95 | 82.18 | 0 |
| 14 | 308.32 | 8 | 3 | 0.15 | 4 | 108.58 | 250.59 | 71.54 | 0 |
| 15 | 317.16 | 6 | 3 | 1.79 | 2 | 90.11 | 226.57 | 77.92 | 0 |
| Pentamidine | 340.43 | 6 | 6 | 1.49 | 10 | 118.22 | 324.60 | 68.22 | 1 |

Table 5: Predicted in silico ADME properties for target compounds, 2, 7, 8, 14 and 15, compared with those of the reference drug Pentamidine.

| Compd. No. | ^a HIA | ^b CaCo-2 | ^c MDCK | ^d PPB | ^e BBB | ^f SkinP |
|------------------|---------------------------|------------------------|-------------------|---------------------|---------------------------|--------------------|
| Acceptable value | 70–100% (good absorption) | >90(high permeability) | | >90% strong binding | >0.40 CNS active compound | ≥-3 |
| 2 | 91.95 | 28.21 | 27.05 | 72.14 | 0.07 | -3.54 |
| 7 | 96.85 | 16.42 | 0.84 | 86.11 | 0.38 | -3.19 |
| 8 | 96.45 | 38.05 | 7.00 | 85.83 | 0.27 | -3.43 |
| 14 | 84.46 | 19.46 | 7.23 | 70.45 | 0.01 | -4.41 |
| 15 | 94.00 | 13.86 | 19.09 | 83.60 | 0.19 | -4.41 |
| Pentamidine | 65.27 | 0.47 | 5.03 | 59.80 | 0.42 | -2.39 |

^a Human intestinal absorption (%). ^bin vitro CaCo cell permeability (nm/sec). ^cin vitro MDCK cell permeability (nm/sec). ^din vitro plasma protein binding (%). ^ein vitro blood–brain barrier penetration (C. brain/ C. blood). ^f Skin permeability

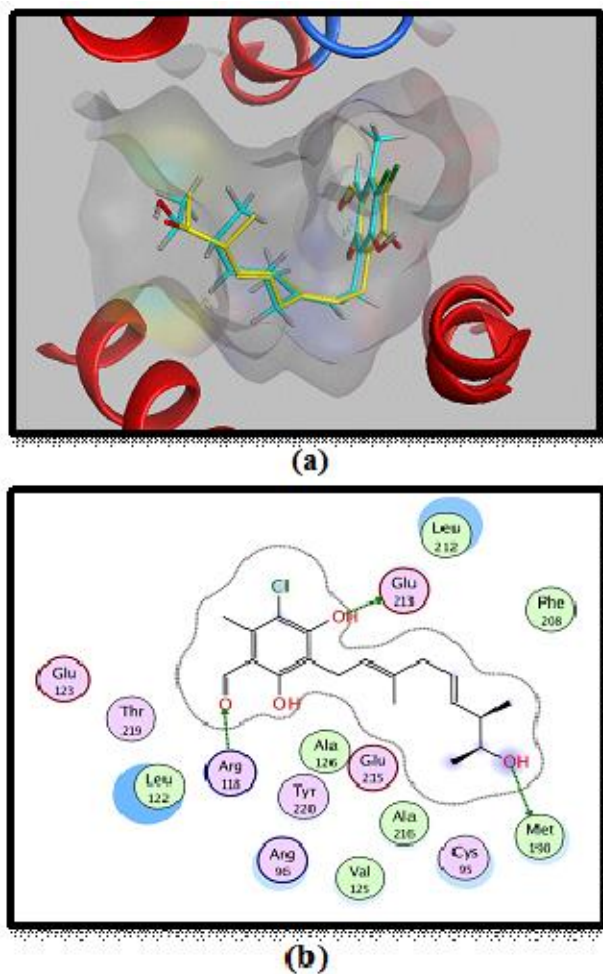


Fig. 8: View of the ligand compound (3-chloro-4,6-dihydroxy-5-[(2E,6E,8S)-8-hydroxy-3,7-dimethylnona-2,6-dien-1-yl]-2-methylbenzaldehyde) in the active site of the target protein (PDB-3VVa) with its amino acid residues: (a) three-dimensional view and (b) two-dimensional view.

Validation for the docking protocol was achieved by docking the co-crystallized ligand. The results obtained revealed that the ligand had a binding energy score of -10.4465 Kcal/mol. It also formed three hydrogen bonding interactions with GLU 213, ARG 118 and MET 190 amino acid residues through two OH and C=O groups (figs. 9-13).

Predicted molecular properties and drug likeness

To further explore drug-likeness properties of the most active derivatives (2, 7, 8, 14 and 15) compared to the reference drug Pentamidine, theoretical calculations for various parameters were conducted, including molecular weight, hydrogen bond acceptors and donors, rotatable bonds, topological polar surface area, molecular volume, absorption percentage and log P "octanol/water" partition coefficient. Results are provided in supplementary data (table 4).

The results showed that all the tested compounds obeyed Lipinski's rule of five with an n-violation value of zero, which is better than that of the reference drug.

In silico ADME prediction

In silico ADME prediction assessed properties such as absorption, distribution, metabolism and excretion for compounds 2, 7, 8, 14 and 15, along with the reference drug Pentamidine. The obtained results are listed in table 4. Results indicated good intestinal absorption values ranging from 84.46 to 96.85% for all target derivatives, surpassing those of the reference drug (65.27%) (table 5). Low-to-moderate permeability results were observed for *in vitro* CaCo-2 and MDCK cells.

DISCUSSION

Biological screening

Antitrypanosomal activity

It should be pointed out that there was a correlation between biological activity and the study of molecular docking. The antitrypanosomal derivative 8 was found to be the most effective one, having the highest binding energy score of -10.2820 Kcal/mol among all tested compounds (Alzahrani *et al.*, 2017).

Antileishmanial activity

Finally, when these results were linked to those that appeared in the docking experiments, it was found that thiopyrimidinone derivatives, 14 and 15 were among the compounds that have a high binding energy score (for compound 14; -14.6970 Kcal/mol) or those that make a large number of hydrogen bonding interactions (for compound 15; eight H-B) and these are the same compounds that have been proven effective (Alkhalidi *et al.*, 2019; Amisigo *et al.*, 2019 and Dias-Lopes *et al.*, 2021).

In silico molecular docking studies

It is worth to mention that presence of only one ester group in the structure of hydrazineylidene derivatives alongside with electron donating groups (3,4-dimethoxy derivatives), as in compound 2, increased the binding interactions inside the active site. Additionally, pyrazolone derivatives with ester group at phenyl *para* position, compound 7, or with 3,4-dimethoxyphenyl part, compound 8, showed the highest energy binding scores. Thiopyrimidinone derivatives 14 and 15 bearing 3,4-dimethoxyphenyl moiety or 3,5-dichlorophenyl ring exerted also high binding interactions. The following pharmacophores OCH₃, pyrazolone C=O and thiopyrimidinone C=S, shared an important role in good fitting inside the enzyme active site through the formation of hydrogen bonding interactions with Thr335, Thr51 and Lys60 amino acid residues.

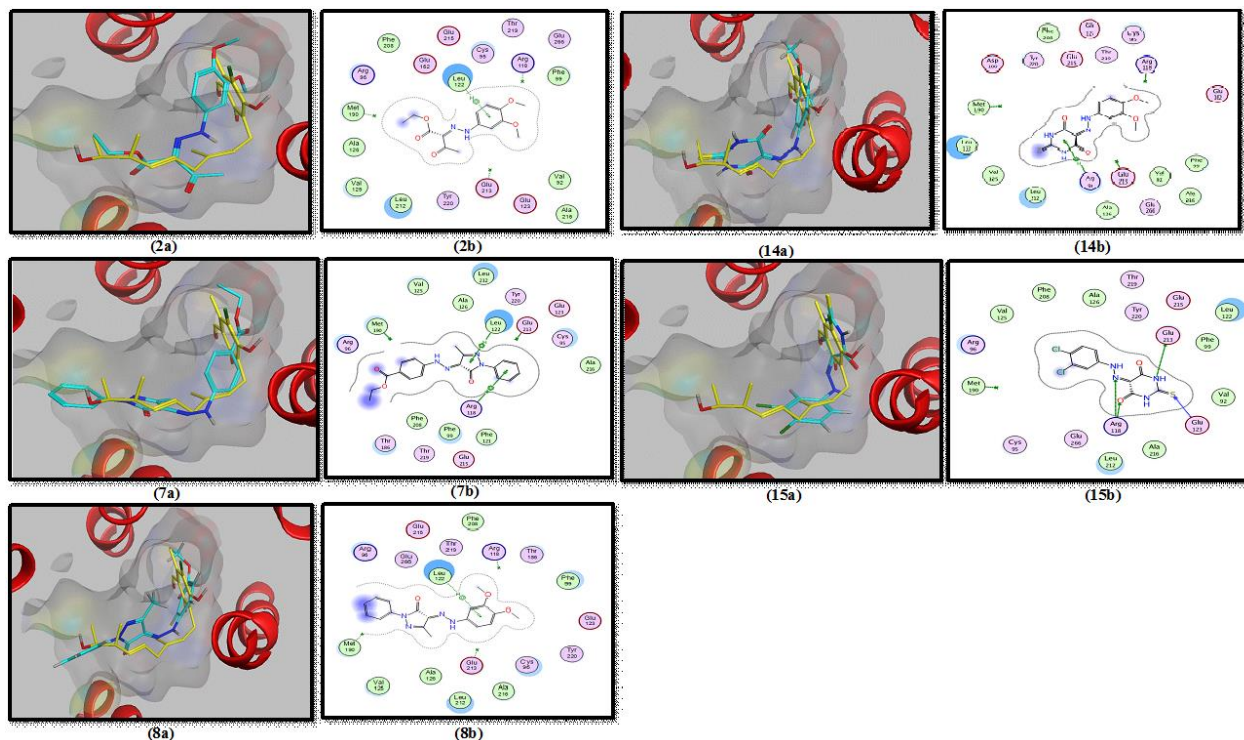


Fig. 9-13: (a) Superimposed view of target compound 2, 7, 8, 14 and 15 (cyan lines) and ligand molecule (yellow lines) in the active site of the target protein. (b) Two-dimensional view of H.B. interactions of compound 2, 7, 8, 14 and 15 and ARG 118, GLU 213 and GLU 123 amino acid residues in the active site of the target protein.

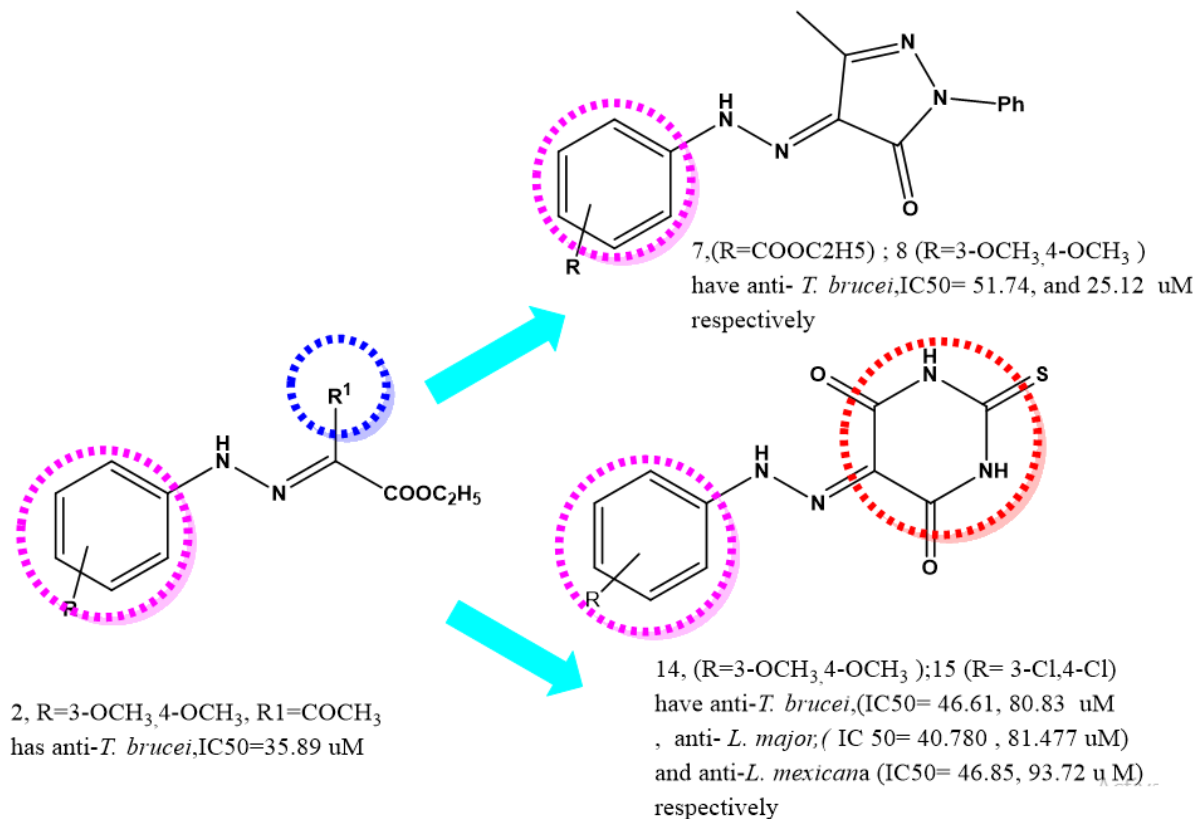


Fig. 14: SAR of Active compounds

By docking the most biologically active derivatives, 2, 7, 8, 14 and 15, it was observed that compound 8 (which was the most potent antitrypanosomal agent among test compounds) had the highest binding energy score nearly equal to the co-crystallized ligand, -10.2820 and formed a pi-H interaction with LEU 122 amino acid residue.

Additionally, the four other derivatives, 2, 7, 14 and 15 displayed one to three binding interactions with LEU 122, ARG 118, ARG 96, GLU 213 and GLU 123 amino acid residues. These derivatives showed binding energy scores ranged from -9.8561 to -7.9950 Kcal/mol.

Finally, we can conclude that the obtained results were in accordance with that obtained from biological *in vitro* assay.

Predicted molecular properties and drug likeness

It was noticeable that active pyrimidine thione derivative 15 resembled the reference drug in its lipophilic character with a log P value of 1.79 for compound 15 and 1.49 for Pentamidine. Moreover, chloro derivative of pyrimidine thione 14 showed an absorption % of 71.54 that was similar to that of the reference drug (68.22) (<https://www.molinspiration.com/>).

A good bound effect on the plasma protein was observed for the target derivatives (86.11-70.45%), which was better than that for Pentamidine (59.80%), which indicated that it might have more prolonged drug action than the reference drug does.

On the other hand, the problems of CNS penetration and permeability that were observed in Pentamidine might be have been overcome in the target compounds, especially for compounds 2 and 14, with blood-brain barrier values of 0.07 and 0.01, respectively. Low skin permeability values were predicted for all the target derivatives, 2, 7, 8, 14 and 15, and they ranged from -4.41 to -3.19. Finally, we can conclude that target derivatives 2, 7, 8, 14, and 15 have good ADME properties (table 5). (<https://preadmet.webservice.bmdrc.org/adme>)

SAR tested compounds

The structures and biological activities of tested compounds are mentioned (in supplementary data fig. 14.) Depending on the chemical structures, biological screening results, and docking studies of the targets synthesized compounds, compound 2 has intermediate anti-trypanosomal activity, which is attributed to interaction with PDB-2JK6 and PDB-3VVa with E-scores = 12.62 and 8.94 Kcal/mol respectively. This is result of dimethoxy groups acting as electron donors, which enhance pi-H interactions (fig. 14).

Also, the ethyl ester (C=O) of compound 7 has a pronounced role in interactions with receptors amino THR 51 and ARG 118 with E-score of 13.38 and -8.99

kcal/mol. THR 51 and ARG 118 are amino acid residues that interact with ligands (table 3).

The compound 8 with two electron-donating groups (3,4-dimethoxy), has the highest activity towards trypanosomal and this was regarding the lowest energy of interactions (-14.52 and -10.22 kcal/mol) and interactions with ASP 327 and LEU 122 (amino acid residues).

Compound 14 with thiobarbituric acid scaffold and 3,4-dimethoxyphenyl showed significant activities against all parasites and potent interactions through amino acid residues (ASP 327 (2.47), LYS 60 (2.63), and ARG 96 (4.02), so the electron-donating dimethoxy groups have marked effects on the interaction, but compound 15 has lower inhibitory activities than compound 14 in spite of the fact that has the thiobarbituric moiety and several interactions with the receptor, but the electron-withdrawn dichloro groups are forced towards weakening these interactions.

Compounds 10, 11, and 12 have a barbituric ring but had no impact on the targets tested. This suggests that the barbituric ring is not favorable for biological activity in this circumstance.

Open Chain Compounds 1 through 6, none of the open chain compounds 1 through 6 have demonstrated inhibitory efficacy against leishmania or trypanosomes, with the exception of compound 2, which exhibited a marginally inhibitive effect on *Trypanosoma*. The SAR analysis thereby pinpoints the precise structural traits and substituents required for these compounds' biological activity against LYS 60, *Trypanosoma*, and *Leishmania*. These findings might be useful in guiding future work on pharmaceutical design and optimization to produce more potent medications for the intended illnesses.

CONCLUSIONS

In this research, all hydrazones, azo-pyrazole, and azopyrimidine compounds were screened to assess their activity against *Leishmania* species and *Trypanosoma brucei*. The results showed that five of the tested compounds showed moderate activity against *Trypanosoma brucei*, with compound 8 displaying the strongest inhibition, closely resembling the activity of the positive control (eflornithine). Additionally, there was a parallel relationship between the molecular docking experiment and the *in vitro* biological activity levels. Moreover, the target derivatives 2, 7, 8, 14 and 15 showed highest binding energy and good drug-likeness and ADME properties if compared to the reference drug. Compounds 8 and 14 not only exhibited promising biological activity but also demonstrated drug-like properties, which are essential for the development of safe and effective pharmaceuticals. Future plan for this work

depending on the significant finding as it suggests that compound 14 may have a dual or broad-spectrum activity against both parasites. Such versatility could be valuable in the development of anti-parasitic drugs, particularly if it exhibits a favorable safety profile and pharmacokinetic properties.

ACKNOWLEDGMENTS

The author would like to express gratitude to Prof. Harry P. de Koning from the College of Medical, Veterinary, and Life Sciences at the University of Glasgow, Glasgow, UK, for facilitating the execution of the experiments described in this study in his laboratory.

REFERENCES

- Abdegawad MA (2019). Synthesis and antibacterial evaluation of new azo-pyrimidine Derivatives. *J. App. Pharm. Sci.*, **9**(suppl1): 9-16.
- Abuzaid AA, Aldahan MA, Helal MAA, Assiri AM and Alzahrani MH (2020). Visceral leishmaniasis in Saudi Arabia: From hundreds of cases to zero. *Acta Trop.*, **212**: 105707.
- Alanazi AD, Alouffi AS, Alyousif MS, Rahi AA, Ali MA, Abdullah HHAM, Brayner FA, Mendoza-Roldan JA, Bezerra-Santos MA and Otranto D (2021). Molecular characterization of Leishmania species from stray dogs and human patients in Saudi Arabia. *Parasitol. Res.*, **120**(12): 4241-4246.
- Alkhalidi AAM, Abdelgawad MA and Youssif BGM (2018). Synthesis, antimicrobial evaluation and docking studies of new pyrazolone derivatives. *Trop. J. Pharm. Res.*, **17**(11): 2235-2241.
- Alkhalidi AAM, Abdelgawad MA, Youssif BGM, El-Gendy AO and De Koning HP (2019). Synthesis, antimicrobial activities and GAPDH docking of new 1, 2, 3-triazole. *Trop. J. Pharm. Res.*, **18**(5): 1101-1108.
- Alkhalidi AAM, De Koning HP and Bukhari SNA (2019). Antileishmanial and antitrypanosomal activity of symmetrical dibenzyl-substituted α , β -unsaturated carbonyl-based compounds. *Drug Des. Dev. Ther.*, **13**: 1179-1185.
- Alzahrani KJH, Ali JAM, Eze AA, Looi WL, Tagoe DNA, Creek DJ, Barrett MP and de Koning HP (2017). Functional and genetic evidence that nucleoside transport is highly conserved in Leishmania species: implications for pyrimidine-based chemotherapy. *Int. J. Parasitol. Drugs Drug Resist.*, **7**(2): 206-226.
- Amisigo CM, Antwi CA, Adjimani JP and Gwira TM (2019) *In vitro* anti-trypanosomal effects of selected phenolic acids on Trypanosoma brucei. *PLOS ONE*, **14**(5): e0216078.
- Bekhit AA, Lodebo ET, Hymete A, Ragab HM, Bekhit SA, Amagase K, Batubara A, Abourehab MAS, Bekhit AEA and Ibrahim TM (2022). New pyrazolylpyrazoline derivatives as dual acting antimalarial-antileishmanial agents: Synthesis, biological evaluation and molecular modelling simulations. *J. Enzyme Inhib. Med. Chem.*, **37**(1): 2320-2333.
- Black SJ and Mansfield JM (2016). Prospects for vaccination against pathogenic African trypanosomes. *Parasite Immunol.*, **38**(12): 735-743.
- Brindha J, Balamurali M and Chanda K (2021). An overview on the therapeutics of neglected infectious diseases-leishmaniasis and Chagas diseases. *Front. Chem.*, **9**: 622286.
- Cayla M, Rojas F, Silvester E, Venter F and Matthews KR (2019). African trypanosomes. *Parasit. Vectors*, **12**(1): 190.
- Chuang H, Huang LCS, Kapoor M, Liao YJ, Yang CL, Chang CC, Wu CY, Hwu JR, Huang TJ and Hsu MH (2016). Design and synthesis of pyridine-pyrazole-sulfonate derivatives as potential anti-HBV agents. *Med.*, **7**(5): 832-836.
- De Rycker M, Baragaña B, Duce SL and Gilbert IH (2018). Challenges and recent progress in drug discovery for tropical diseases. *Nature*, **559**(7715): 498-506.
- Dias-Lopes G, Zabala-Peñañiel A, de Albuquerque-Melo BC, Souza-Silva F, Menaguali do Canto L, Cysne-Finkelstein L and Alves CR (2021). Axenic amastigotes of Leishmania species as a suitable model for *in vitro* studies. *Acta Trop.*, **220**: 105956.
- Dize D, Tata RB, Keumoe R, Kouipou Toghueo RM, Tchataat MB, Njanpa CN, Tchuengui VC, Yamthe LT, Fokou PVT, Laleu B, Duffy J, Bishop OT and Boyom FF (2022). Preliminary structure-activity relationship study of the MMV pathogen box compound MMV675968 (2,4-diaminoquinazoline) unveils novel inhibitors of Trypanosoma brucei brucei. *Molecules*, **27**(19): 6574.
- Dumoulin PC and Burleigh BA (2018). Stress-induced proliferation and cell cycle plasticity of intracellular Trypanosoma cruzi amastigotes. *mBio.*, **9**(4): 4.
- Franco JR, Simarro PP, Diarra A and Jannin JG (2019). Epidemiology of human African trypanosomiasis. *Parasites Vectors*, **12**: 190.
- Ghatee MA, Taylor WR and Karamian M (2020). The geographical distribution of cutaneous leishmaniasis causative agents in Iran and its neighboring countries, A review. *Front. Public Health*, **8**: 11.
- Giordani F, Morrison LJ, Rowan TG, De Koning HP and Barrett MP (2016). The animal trypanosomiasis and their chemotherapy: A review. *Parasitology*, **143**(14): 1862-1889.
- Hafez HN, El-Gazzar ABA and Al-Hussain SA (2016). Novel pyrazole derivatives with oxa/thiadiazolyl, pyrazolyl moieties and pyrazolo[4,3-d]-pyrimidine derivatives as potential antimicrobial and anticancer agents. *Bioorg. Med. Chem. Lett.*, **26**(10): 2428-2433.
- Hirumi H and Hirumi K (1989). Continuous cultivation of Trypanosoma brucei blood stream forms in a medium

- containing a low concentration of serum protein without feeder cell layers. *The Journal of parasitology*, pp.985-989.
- Insuasty B, Ramírez J, Becerra D, Echeverry C, Quiroga J, Abonia R, Robledo SM, Vélez ID, Upegui Y, Muñoz JA, Ospina V, Nogueras M and Cobo J (2015). An efficient synthesis of new caffeine-based chalcones, pyrazolines and pyrazolo[3,4-b][1,4]diazepines as potential antimalarial, antitrypanosomal and antileishmanial agents. *Eur. J. Med. Chem.*, **93**: 401-413.
- Karrouchi K, Radi S, Ramli Y, Taoufik J, Mabkhot YN, Al-Aizari FA and Ansar M (2018). Synthesis and pharmacological activities of pyrazole derivatives: A review. *Molecules*, **23**(1): 134.
- Khan MAA, Faisal K, Chowdhury R, Nath R, Ghosh P, Ghosh D, Hossain F, Abd El Wahed A and Mondal D (2021). Evaluation of molecular assays to detect *Leishmania donovani* in Phlebotomus argentipes fed on post-kala-azar dermal leishmaniasis patients. *Parasit. Vectors*, **14**(1): 465.
- Khan TA, Mnasri A, Al Nasr IS, Ozdemir I, Gürbüz N, Hamdi N and Koko W (2023). Activity of benzimidazole derivatives and their N-heterocyclic carbene silver complexes against leishmania major promastigotes and amastigotes. *Biointerface Res. Appl. Chem.*, **13**(2): 3-135,
- Kourbeli V, Chontzopoulou E, Moschovou K, Pavlos D, Mavromoustakos T and Papanastasiou IP (2021). An overview on target-based drug design against kinetoplastid protozoan infections: Human African trypanosomiasis, Chagas disease and leishmaniasis. *Molecules*, **26**(15): 4629.
- Li YR, Li C, Liu JC, Guo M, Zhang TY, Sun LP, Zheng CJ and Piao HR (2015). Synthesis and biological evaluation of 1,3-diaryl pyrazole derivatives as potential antibacterial and anti-inflammatory agents. *Bioorg. Med. Chem. Lett.*, **25**(22): 5052-5057.
- Meng FJ, Sun T, Dong WZ, Li MH and Tuo ZZ (2016). Discovery of novel pyrazole derivatives as potent neuraminidase inhibitors against influenza H1N1 virus. *Arch. Pharmazie.*, **349**(3): 168-174.
- Navarro M, Justo RMS, Delgado GYS and Visbal G (2021) Metallo drugs for the treatment of trypanosomatid diseases: Recent advances and new insights. *Curr. Pharm. Des.*, **27**(15): 1763-1789.
- Nayak N, Ramprasad J, and Dalimba U (2015) New INH-pyrazole analogs: Design, synthesis and evaluation of antitubercular and antibacterial activity. *Bioorg. Med. Chem. Lett.*, **25**(23): 5540-5545.
- Oldenburg SH, Buisson L, Beneyton T, Pekin D, Thonnus M, Bringaud F, Riviere L and Baret JC (2021) Confining *Trypanosoma brucei* in emulsion droplets reveals population variabilities in division rates and improves in vitro cultivation. *Sci. Rep.*, **11**(1): 18192.
- Oliveira SS, Ferreira CS, Branquinha MH, Santos AL, Chaud MV, Jain S, Cardoso JC, Kovacevic AB, Souto EB and Severino P (2021) Overcoming multi-resistant leishmania treatment by nanoencapsulation of potent antimicrobials. *J. Chem. Technol. Biotechnol.*, **96**(8): 2123-2140.
- Ramírez-Prada J, Robledo SM, Vélez ID, Crespo MDP, Quiroga J, Abonia R, Montoya A, Svetaz L, Zacchino S and Insuasty B (2017). Synthesis of novel quinoline-based 4,5-dihydro-1H-pyrazoles as potential anticancer, antifungal, antibacterial and antiprotozoal agents. *Eur. J. Med. Chem.*, **131**: 237-254.
- Rasheed Z, Ahmed AA, Salem T, Al-Dhubaibi MS, Al Robaee AA and Alzolibani AA (2019). Prevalence of *Leishmania* species among patients with *Cutaneous leishmaniasis* in Qassim province of Saudi Arabia. *BMC Public Health*, **19**(1): 384.
- Rivas F, Del Mármol C, Scalse G, Pérez-Díaz L, Machado I, Blacque O, Medeiros A, Comini M and Gambino D (2022). New multifunctional Ru(II) organometallic compounds show activity against *Trypanosoma brucei* and *Leishmania infantum*. *J. Inorg. Biochem.*, **237**: 112016.
- Santos SS, de Araújo RV, Giarolla J, Seoud OE and Ferreira EI (2020) Searching for drugs for Chagas disease, leishmaniasis and schistosomiasis: A review. *Int. J. Antimicrob. Agents*, **55**(4): 105906.
- Tihon E, Imamura H, Van den Broeck F, Vermeiren L, Dujardin JC and Van Den Abbeele J (2017). Genomic analysis of isometamidium chloride resistance in *Trypanosoma congolense*. *Int. J. Parasitol. Drugs Drug Resist.*, **7**(3): 350-361,
- Verbitskiy EV, Rusinov GL, Charushin VN and Chupakhin ON (2019) Development of new antituberculosis drugs among of 1,3- and 1,4-diazines. Highlights and perspectives. *Russ. Chem. Bull.*, **68**(12): 2172-2189.
- World Health Organization (2020). Trypanosomiasis, human African (sleeping sickness). World Health Organization, Geneva, pp.103-215.
- World Health Organization (1998). Rappaport sur la Sante´ dans Monde, Geneva, pp.49-56.